Check for updates

Mechanoenzymatic hydrolysis of cotton to cellulose nanocrystals†

Sandra Kaabel, [ID] *[a,b] Inge Schlapp-Hackl,[b] Eero Kontturi [ID] [b] and
Mauri A. Kostiainen [ID] [b]

Solid-state mechanoenzymatic approaches for the production of cellulose nanocrystals from cotton were examined using three commercially available cellulase systems from *Trichoderma reesei*, *Aspergillus niger* and a Cellic CTec2 cellulase blend. A rapid and sharp drop in the degree of polymerization, together with the proportional increase in cellulose crystallinity and generation of nanoscale particles, indicates that cotton is extensively transformed to cellulose nanocrystals with just 15 minutes of ball milling of cotton in the presence of the cellulase enzymes. Subsequent aging of the solid reaction mixture at 55 °C did not significantly affect the degree of polymerization, but resulted in higher material losses due to the increased production of glucose. These results reveal that the endo-activity of the commercial cellulase preparations on cellulose is particularly efficient in solid reaction mixtures (solid loading 50 wt%), allowing for a rapid acid-free generation of cellulose nanocrystals with as low as 0.085 wt% enzyme loading.

Introduction

Cellulose yields valuable renewable nanostructured materials, cellulose nanofibers (CNFs) and cellulose nanocrystals (CNCs), through mechanical, chemical and/or enzymatic processing.[1] Because of the high tensile strength, high aspect ratio and tuneable surface chemistry, cellulose nanomaterials have a strong impact on the properties of composites, films, foams, fibres and emulsions, which has quickly led to an increased demand across industries.[2] Food and beverage, textile and personal care industries are, for example, driving the demand due to the wide applicability of nanocelluloses in sustainable packaging solutions.[3,4] The nanocellulose market is projected to grow from USD 0.34 billion in 2022 to USD 3.38 billion by 2032 with a forecast compound annual growth rate (CAGR) of 23.9%, based on the market analysis report carried out by Global Market Insights Inc (2023). This increased demand is, however, met with some persistent challenges in nanocellulose production. Mechanical CNF production processes are energy intensive,[5] while industrial production of CNCs generally relies on a large amount of hazardous concentrated acids,[6,7] which need to be recycled or disposed of.[8] Furthermore, acid hydrolysis, particularly with sulphuric acid, can lower the ther-

mostability of the obtained CNCs through chemical modification.[8,9] Enzyme-mediated extraction of nanocelluloses, on the other hand, proceeds under milder reaction conditions, retains the native surface chemistry of cellulose and does not generate harmful waste.[10,11] Cellulase enzymes, consisting of endoglucanases (EG, EC 3.2.1.4), cellobiohydrolases (CBH, EC 3.2.1.91), and β-glycosidases (BG, EC 3.2.1.21), which synergistically hydrolyse the β-1,4-glucosidic bonds of cellulose, have been applied to facilitate chemical or mechanical processing of cellulose[11] or as the main step in nanocellulose production.[12–28] For the former, the precise role of enzymes can be difficult to pick apart, for example in a common case when the enzymatic hydrolysis step is carried out on microcrystalline cellulose, which consists of crystalline cellulose with a low degree of polymerization (DP) generally obtained through acid hydrolysis. In such systems, the morphology of the resulting nanomaterials obtained from enzymatic treatment is presumably strongly influenced by the hydrolytic extent of the starting microcrystalline cellulose. Studies reporting enzymatic hydrolysis as the main step for converting high DP cellulosic materials (*e.g.* wood-sourced cellulose or cotton linters) to nanocrystals, however, are generally carried out in dilute aqueous solutions (1–2 wt% solid loading) and report long reaction times (24–72 h) and modest CNC yields (*ca.* 10%). Meanwhile, mechanochemical and related solid-state approaches have delivered efficient methods to depolymerize cellulose to glucose and water-soluble oligomers, through enzymatic hydrolysis[29–32] or acid hydrolysis,[33–42] by grinding solid reactants in the absence of bulk solvents. Such approaches can accelerate the enzymatic and chemical reac-

[a]Department of Chemistry and Material Science, Aalto University, 02150 Espoo, Finland. E-mail: sandra.kaabel@aalto.fi
[b]Department of Bioproducts and Biosystems, Aalto University, 02150 Espoo, Finland
†Electronic supplementary information (ESI) available: Full experimental details, characterization protocols and data tables. See DOI: https://doi.org/10.1039/d4gc05113k

tions, which take place in the highly concentrated and mechanically agitated solid reaction mixtures.[43,44] Mechanochemical methods can be especially valuable for the production and refining of cellulose nanomaterials, by minimizing the waste generated and the energy consumed by heating the aqueous media in dilute reaction mixtures.[24,45,46]

The objective of the present work was to investigate the feasibility of obtaining cellulose nanocrystals from cotton linters by employing mechanoenzymatic approaches in the presence of commercially available enzymes, focusing on the interplay of cellulase enzymes in the highly concentrated reaction settings (50% w/v) under different ball milling and aging conditions. Following the release of glucose and the recovery of hydrolysed cellulose, the analysis of cellulose molecular mass and morphology after milling and during aging provides a systematic picture of the action of three different commercial cellulase mixtures on cotton cellulose, culminating in a rapid low-waste and acid-free method to generate CNCs.

Results and discussion

Cellulose substrates and enzymatic hydrolysis

Raw cotton balls (CB), without pre-treatment or further purification steps, were powdered to <600 μm particles using a Wiley knife mill. Cellulose fibres remained intact upon pre-milling, providing a minimally processed substrate (DP_n = 924 ± 19, DP_w = 1518 ± 22, $Đ$ = 1.64 ± 0.01) in comparison to commercially available microcrystalline cellulose, which is often used as a starting material for enzymatic hydrolysis,[47–50] but represents an acid-processed low DP cellulose (DP_n = 102, DP_w = 282, $Đ$ = 2.8) containing micron-scale particles (Fig. S1†). To facilitate comparisons with benchmarked CNCs,[51,52] powdered Whatman 1 filter paper (FP) was also studied as a substrate here (DP_n = 656 ± 8, DP_w = 1089 ± 23, $Đ$ = 1.66 ± 0.06), as it is commonly used in lab-scale sulphuric acid and HCl-gas CNC production protocols. The hydrolytic reactions were carried out using a mechano-enzymatic approach,[44,53,54] in which cellulose powder is ball milled in the presence of the enzyme and a small amount of buffer (100 mM NaPB, pH 6) at a liquid-to-solid ratio η = 1.0 μL mg^{-1}, i.e., a solid loading of 50 wt%. The buffer provides the hydrolysis substrate (≈11 molar equivalents of water to anhydrous glucose unit), enzyme buffering media, and reaction lubricant assisting molecular collisions. Mechanochemical liquid-assisted grinding (LAG) reactions, by ball milling or extrusion, are often faster than conventional solution reactions due to enhanced mixing at high concentrations.[55–57] The amount of the buffer used here fully absorbs the cotton substrate, resulting in moist solid reaction mixtures. The action of commercially available cellulase systems from *Trichoderma reesei* (*Tr*), *Aspergillus niger* (*An*) and a Cellic CTec2 blend was compared after a brief period of ball milling (15 or 30 minutes) and after subsequent static incubation (24 or 72 hours of aging at 55 °C), with the extent of enzymatic hydrolysis monitored by quantifying the released

glucose and by characterization of the recovered hydrolysed cellulose.

Glucose yield as a measure of the hydrolysis extent of cotton

Influential mechanoenzymatic reaction parameters with respect to the type of cellulase preparation – the type of buffer, enzyme loading, liquid-to-solid ratio, and reaction duration – were screened based on glucose assays, which represents the hydrolysis end-product, after hydrolysis of cellulose by endo-glucanases and cellobiohydrolases followed by cellobiose hydrolysis to glucose by β-glucosidase.[58] Regardless of the cotton material or the type of cellulase used, the amount of glucose released was negligible after a short 15 minute milling step (Fig. 1b, at 0 h of aging) and gradually increased during the aging period. At a concentration of 15 U g^{-1} cellulose, the *Tr* cellulases proved to be the most active, producing 20–25% yield of glucose from both cellulose materials within 72 hours. When applied at a comparable concentration (U g^{-1}), the glucose production with *An* was below 10% regardless of the cotton source, while CTec2 cellulases appeared sensitive to the cellulose source, resulting in *ca.* 20% yield of glucose from CBs and 12% from FP (Fig. 1b, data in Tables S1 and S3†). Therefore, further reaction parameters were screened using *Tr* cellulases. This revealed that varying the buffer type (100 mM NaPB at pH 6, 50 mM citrate at pH 6, 50 mM NaOAc at pH 5 or H$_2$O), the liquid-to-solid ratio (1.0–2.0 μL mg^{-1}) and the initial milling duration (5–30 min) had a small effect on the amount of glucose obtained in 72 hours (Fig. 1d, e and f, respectively, Table S2†), while increasing the enzyme loading (1.6 to 8.2 wt%) led to much higher glucose yields (Fig. 1c and Table S1†).

Hydrolysis extent based on recovered hydrolysed cellulose

Given the likely variation in the relative activity of the cellulase enzymes (EG, CBH and BG) within the commercial *Tr*, *An* and CTec2 enzyme preparations, the correlation between the glucose yield and the yield of cellulose nanocrystals (CNCs) is not straightforward. Higher glucose yields, which are associated with higher weight losses, are not optimal for reaching a high yield of CNCs, as ideally CNCs would be obtained by controlled partial hydrolysis of cotton fibres with minimal material loss. Therefore, to identify the reaction conditions favouring partial hydrolysis of cellulose to CNCs, the bulk hydrolysed cellulose from the reactions with identified influential variables (cellulase mixture type and loading) was characterized at different timepoints by gel-permeation chromatography (GPC), powder X-ray diffraction (PXRD) and atomic force microscopy (AFM), to determine the hydrolysis degree (DP_n, DP_w and $Đ_M$), the changes in cellulose crystallinity (CrI) and the morphology of the hydrolysed cellulose, respectively.

Isolation of hydrolysed cellulose

Isolation of hydrolysed cellulose from water-soluble hydrolysis products could be easily achieved by washing the solids with either water or ethanol. However, these conditions were not successful in removing the enzymes, which remained
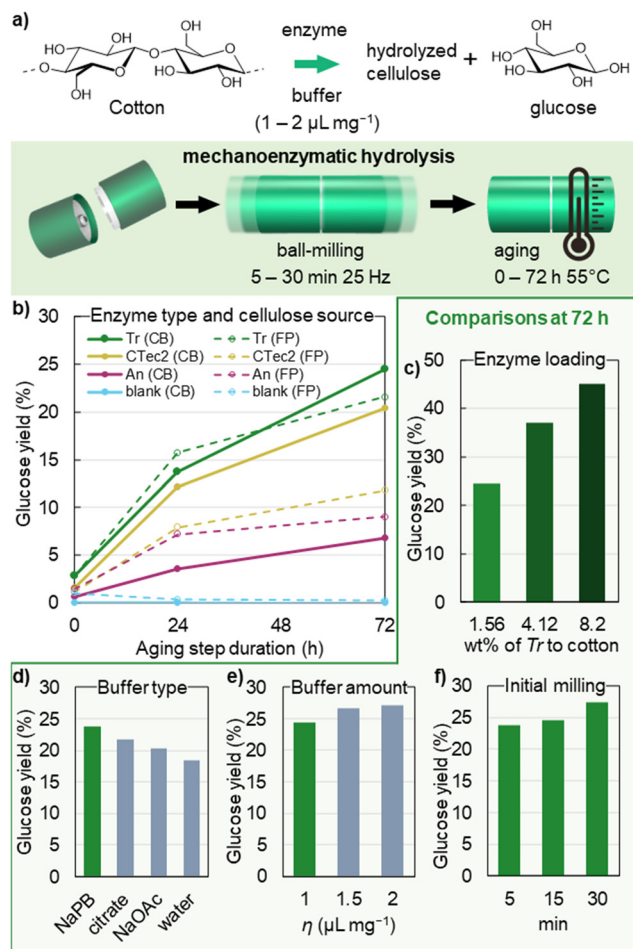
Fig. 1 (a) General reaction scheme for the mechanoenzymatic hydrolysis of cotton (CB – cotton balls, FP – Whatman 1 filter paper), combining a brief period of ball milling with subsequent aging. (b) Glucose yields from studied cotton sources: right after milling (0 h), and after subsequent aging for 24 or 72 h at 55 °C, by comparing *Trichoderma reesei* (*Tr*), *Aspergillus niger* (*An*) and Cellic CTec2 cellulase enzymes to a blank reaction. Enzyme loading for *Tr*, *An* and CTec2 was adjusted based on respective activity (see the ESI†), to 1.56 wt% for *Tr*, 0.085 wt% for *An* and 0.305 wt% for CTec2. Note that the enzyme loading (wt%) is based on all proteins contained in the cellulase preparation (see the ESI†). (c–f) Glucose yield from CB after ball milling + 72 h of aging, by varying the enzyme loading (c), the type of buffer (d), the amount of buffer (e) and the initial milling duration (f). Unless the specific parameter was varied, the base conditions for (c–f) were 400 mg of CB, 1.56 wt% of *Tr*, NaPB (100 mM, pH 6, η = 1.0 μL mg^{-1}), 15 min of ball milling and 72 h of aging at 55 °C.

adsorbed to the solid material. Therefore, alternative cellulose washing conditions were tested based on a reported pH-triggered cellulase desorption protocol (see the ESI† for details, recovered cellulose amounts given in Table 1).[59] Gently stirring the crude reaction mixture at 1 wt% for 1 hour in a pH adjusted 50 mM citrate buffer (pH 10), followed by filtration on a 0.22 μM nylon filter removed up to 40% of the proteins depending on the cellulase preparation type and aging duration. A clear correlation could be observed between decreased removal efficiency and duration of the aging step, with a

bigger proportion of cellulases removed right after milling (7% *Tr*, 40% *An* and 15% CTec2), compared to that after 24 h (≤10% *Tr* and CTec2, 25% *An*) and 72 h (≤5% *Tr* and CTec2, 20% *An*) of aging. This shows that cellulases proceeding furthest in the hydrolysis of cellulose to glucose are tightly bound, resulting in lower desorption of the enzymes (confirmed by elemental analysis, see Table S5†). This is consistent with earlier observations that some cellulases adsorb to cellulose surfaces nearly irreversibly,[60] which implies that a longer hydrolysis duration leads to lower enzyme recyclability and increased protein impurities in the recovered hydrolysed cellulose.

Degree of polymerization of hydrolysed cellulose

Reactions in the absence of cellulases did not lead to any significant changes in the degree of polymerization of cotton (Fig. 2b and c), showing that cellulose is not hydrolysed solely by the reaction conditions applied. A rapid decrease in cellulose molecular mass was observed, however, when the cotton materials were exposed to cellulases under these conditions (Fig. 2b and d–f). Within the initial 15 minutes of ball-milling, the number average degree of polymerization (DP_n) of cellulose drops by 50–75% (Fig. 2b and Table 1, entries 5, 8 and 11), indicating that endoglucanases, which cleave glycosidic bonds at disordered points mid-chain,[61] are particularly active under mechanically agitated moist-solid reaction conditions, rapidly producing shorter polymers. Similar DP_n values obtained after the milling step indicate that endo-activity on cellulose is comparable in the three cellulases tested. A limited decrease in DP_n during subsequent aging (Table 1 entries 6, 7, 9, 10, 12 and 13) allows us to conclude that easily accessible parts of cellulose fibres (less-ordered and exposed) are enzymatically hydrolysed already with the initial short milling step. Previously, mixing[24,62] or extrusion[63] of dissolving pulp at a solid loading of 20–30 wt% in the presence of endoglucanases was shown to strongly enhance the hydrolytic action of cellulase enzymes, owing to fibre–fibre friction at a low water content, leading to a 54% drop in the pulp molar mass and the disruption of the microfibril structure during 2 hours of treatment. This provided access to low-DP pulp for improved dissolution in NaOH/ZnO in the Biocelsol process,[63] and showcased the potential of enzymes for the sustainable production of microfibrillated and nanoscale cellulose materials from the pulp in the HefCel process.[24] Our results, on one hand, clearly support this finding and furthermore show that enzymatic treatments at an even higher solid loading (50 wt%) can be achieved by brief ball-milling, yielding a dramatic 75% drop in DP_n within 15 minutes, using a commercial cellulase preparation (*Tr* or *An* cellulases). *An* cellulases appear to have particularly high endo-activity, leading to a low DP_n at a significantly lower enzyme loading (0.085 wt%) compared to *Tr* cellulases (1.56 wt%), and compared to the cellulase preparation applied in the HefCel process (0.6 wt%).[24] For all three cellulase preparations tested here, the decrease in the weight average degree of polymerization DP_w was smaller (15–45%) compared to the drop in DP_n, leading to an increase in the dis-

Table 1 Summary of the varying mechanoenzymatic reaction conditions and properties of the isolated hydrolysed cellulose, the same for all reactions: the starting material (CB = cotton balls, FP = Whatman 1 filter paper) was pre-milled (with a 30-mesh screen), the buffer was 100 mM sodium phosphate (pH 6), introduced at 1.0 μL mg^{-1}. The average of two measurements is given for each sample in GPC analysis, and the measurement deviation is given in the ESI (Tables S1 and S4†)

Entry	Cotton & enzyme	Enzyme loading	Hydrolysis conditions	Recovered cellulose %	DP_n [a]	DP_w [a]	$Đ$ (M_w/M_n) [b]	CrI (CI) %
1	CB start	N/A	None	N/A	920	1520	1.6	66 (62)
2	CB + blank	0 wt%	15 min + 0 h	91	1300	1720	1.3	ND
3	CB + blank	0 wt%	15 min + 24 h	90	1070	1565	1.5	ND
4	CB + blank	0 wt%	15 min + 72 h	94	1130	1620	1.4	ND
5	CB + *Tr*	1.6 wt%	15 min + 0 h	91	290	1100	4.0	71 (69)
6	CB + *Tr*	1.6 wt%	15 min + 24 h	77	280	950	3.5	76 (73)
7	CB + *Tr*	1.6 wt%	15 min + 72 h	68	260	1050	4.0	77 (76)
8	CB + *An*	0.085 wt%	15 min + 0 h	100	290	1220	4.2	72 (72)
9	CB + *An*	0.085 wt%	15 min + 24 h	86	240	1040	4.4	74 (73)
10	CB + *An*	0.085 wt%	15 min + 72 h	93	300	1010	3.4	75 (74)
11	CB + CTec2	0.3 wt%	15 min + 0 h	94	450	1290	2.9	72 (69)
12	CB + CTec2	0.3 wt%	15 min + 24 h	80	250	820	3.3	74 (76)
13	CB + CTec2	0.3 wt%	15 min + 72 h	76	290	1150	4.0	78 (77)
14	CB + *Tr* (4.1 wt%)	4.1 wt%	15 min + 72 h	61	360	1280	3.6	ND
15	CB + *Tr* (8.2 wt%)	8.2 wt%	15 min + 72 h	49	510	1410	2.8	ND
16	CB + *Tr*	1.6 wt%	30 min + 0 h	100	340	980	2.9	ND
17	CB + *Tr*	1.6 wt%	30 min + 24 h	80	185	645	3.5	ND
18	CB + *Tr*	1.6 wt%	30 min + 72 h	68	205	620	3.0	ND
19	FP start	N/A	none	N/A	655	1090	1.7	ND
20	FP + blank	0 wt%	15 min + 0 h	92	580	1000	1.7	ND
21	FP + blank	0 wt%	15 min + 24 h	92	500	970	1.9	ND
22	FP + *Tr*	1.6 wt%	15 min + 0 h	88	250	720	2.9	ND
23	FP + *Tr*	1.6 wt%	15 min + 24 h	74	360	1040	2.9	ND

[a] The degree of polymerization is given as the average of two measurements. Measurement deviation, which was up to 20%, is included in ESI Tables S1 and S4.† [b] Dispersity, given as the average of two measurements.

persity of cellulose to $Đ(M_w/M_n)$ = 3–4 when compared to the cotton starting materials (Fig. 2b). A similar increase in dispersity is observed in the acid-catalyzed production of CNCs from cotton.[7,64] A shift in the molecular mass distribution (Fig. 2c–f) of cellulose to a lower M_w by mechanoenzymatic reactions here follows the activity trends observed in glucose assays – with the most pronounced shift observed for *Tr* upon aging, followed by CTec2 and the least pronounced shift observed for *An*. Notably, increasing the loading of the *Tr* enzyme, to either 4.2 or 8.2 wt%, did not bring a larger decrease of the DP_n or DP_w of cellulose (Table 1, entries 11 and 12). The resulting bimodal molecular mass distributions (Fig. 2g, 72 h data shown) rather indicate that a larger amount of long polymer chains is retained, compared to when less enzyme is used. This may be explained by the presence of excess cellobiohydrolase enzymes at high enzyme loading. Cellobiohydrolase enzymes are responsible for the processive hydrolysis of cellulose from chain ends, and strong non-productive binding of these enzymes along the cellulose fibre can interrupt the action of endo-active hydrolases,[65,66] leading to retention of longer cellulose chains. Mechanoenzymatic reactions have been shown to benefit from longer or intermittent milling of the reaction mixture, which improves the mixing of the solids and can aid in the exposure of new polymer surfaces for productive enzyme adsorption.[29–31,67–69] Increasing the initial milling duration from 15 to 30 minutes led to a comparable *ca.* 75% drop in DP_n (Table 1, entries 5 and 16), showing that increasing the milling time does not directly impact the DP_n

obtained. However, following the DP over the course of the aging step showed that longer initial milling led to lower DP_n and DP_w after aging (Table 1, entries 17 and 18), indicating that the activity of both cellobiohydrolases and endoglucanases benefit from the improved mixing before the aging step. A rapid drop in the DP_n and DP_w was also observed when FP was exposed to *Tr* cellulases during 15 minutes of ball milling (Fig. 2h), implying rapid and extensive mid-chain hydrolysis of cellulose from either source which allows for the isolation of CNCs.

Structure, properties and particle size of isolated hydrolysed cellulose

X-ray diffraction analysis of bulk isolated enzymatically treated materials after milling (15 minutes of milling, denoted on the graphs as 0 h of aging) and after milling + aging (24 and 72 h) shows that the crystalline structure of cellulose I_β is well preserved (Fig. S2†). In fact, the crystallinity of cellulose increased by *ca.* 10% relative to the starting material (Fig. 3b) already with the brief enzymatic treatment during ball milling, with a further slower increase observed upon subsequent aging for 24 or 72 h. Crystallinity indices based on the Segal peak height method (CrI, Fig. 3a)[70] and the peak fitting method (CI, Fig. 3a) are reported here to give an estimate of the relative changes in crystallinity compared to the starting material (CBs) under different reaction conditions. Neither should be taken as the absolute quantity of crystalline fractions in the materials.[71,72] An equally sharp increase in crystallinity (CrI)
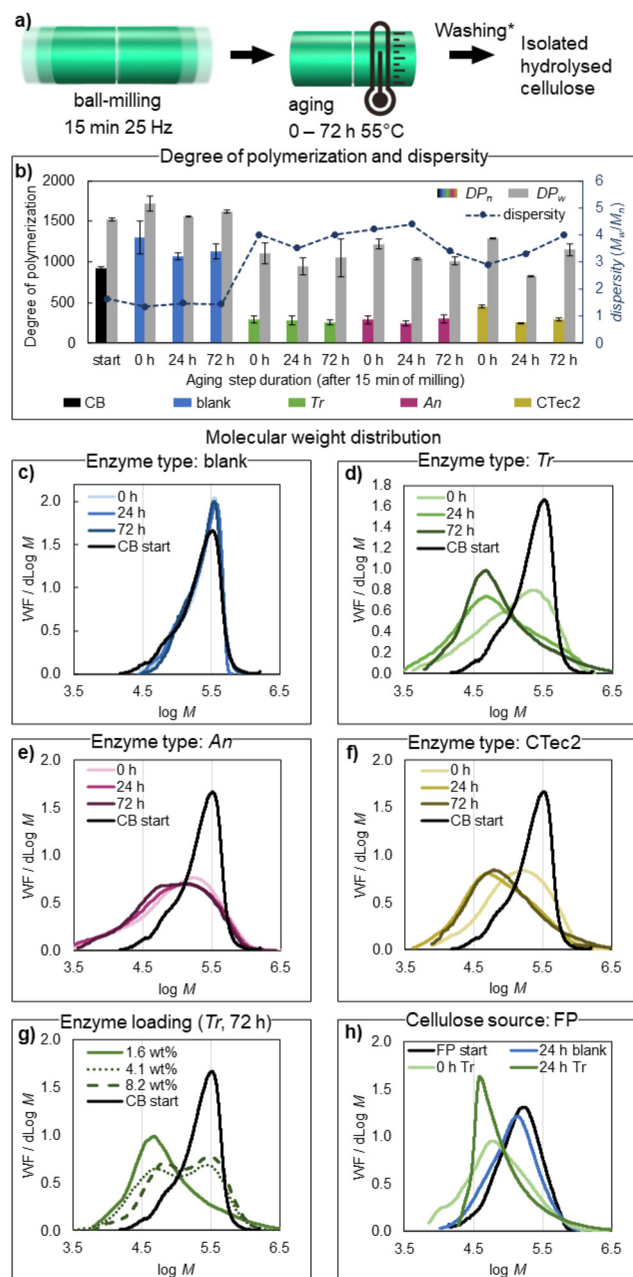
Fig. 2 (a) Scheme of the isolation of hydrolysed cellulose, where washing (*) denotes the removal of the soluble hydrolysis products, and pH-triggered enzyme desorption carried out by stirring the crude reaction mixture for 1 hour at 1 wt% in a pH-adjusted 50 mM citrate buffer (pH 10), followed by washing with a 0.22 μM nylon filter, see the ESI† for details. (b) Number average (DP_n) and weight average (DP_w) degrees of polymerization and dispersity Đ (M_w/M_n) of the isolated hydrolysed cellulose, right after milling (0 h), and after subsequent aging for 24 or 72 h at 55 °C, by comparing *Trichoderma reesei* (*Tr*), *Aspergillus niger* (*An*) and Cellic CTec2 enzymes to a blank reaction. A line is drawn connecting the independent dispersity data points to guide the eye. Each sample was measured twice, and error bars represent the measurement variation. Reactions with the *Tr* enzyme were carried out in triplicate, and the respective error bars represent the experimental standard deviation. (c–h) Molecular mass M_w distribution of the isolated hydrolysed cellulose from reactions with the identified influential variables: enzyme type (c–f), enzyme loading (f) and cellulose source (h), compared to the respective starting material. Full experimental details of the reactions are given in Table S1.†

from 66% to 71–72% for all three tested enzymes, observed right after milling, coincides with the sharp levelling off in DP_n, as observed by GPC, showing the action of endoglucanases preferentially hydrolysing the disordered parts of cellulose fibres. A further increase in sample crystallinity by aging for 24 or 72 h is likely due to the generation and removal of soluble hydrolysis products from cellulose, as the magnitude of the CrI change for *Tr* (77%), *An* (75%) and CTec2 (78%) correlates well with the respective glucose production. Similar to previous reports on enzymatic CNC production,[17] the hydrolysed materials isolated retain the native surface chemistry of cellulose (a zeta potential of up to −26 mV, Fig. 3c), which does not provide enough charge repulsion to obtain good dispersion of the particles in water. This contrasts with CNCs obtained from *e.g.* sulfuric and phosphoric acid hydrolysis or by involving TEMPO-oxidation post-treatment, where negatively charged functional groups are installed to CNC surfaces (resulting in zeta potentials of −35 mV and lower), which enables good dispersion of the particles through electrostatic repulsion.[6,7,73] Cellulose treated with *An* and CTec2 enzymes retain similar zeta potentials of −26.3 ± 0.87 mV (*An*) and −22.2 ± 0.6 mV (CTec2) to the starting material with a value of −24.9 ± 0.7 mV (pre-milled CB); however, the *Tr* treated sample has a distinctly different zeta potential of −16.6 ± 0.2 mV (*Tr*). A similar variation in the resulting zeta potential arising from the enzymatic mixture used was observed in the hydrolysis of eucalyptus cellulose pulp.[74] Here, the variation likely reflects the inefficient removal of the *Tr* enzymes upon product isolation (washing buffer, pH 10), which remain on the surface of the product to a larger extent compared to the *An* and CTec2 cellulases, due to the higher enzyme loading. An earlier onset of thermal degradation (276 °C) and reduced mass loss (71%) of the *Tr*-treated material upon heating, compared to the materials treated with *An* (onset 334 °C, mass loss 90%), CTec2 (onset 335 °C, mass loss 92%), and a pure buffer without enzymes (onset 323 °C, mass loss 92%), also point to a higher amount of protein impurities in the *Tr* sample (Table S6† and Fig. 3d), as an increase of active groups on the surface of CNCs can impact the thermal degradation of cellulose. All mechanoenzymatically obtained materials have higher thermal stability compared to sulfate-CNCs (onset 160 °C) and phosphate-CNCs (onset 207 °C) obtained from acid hydrolysis,[73] and similar stability to enzymatically obtained CNCs (onset 205–316 °C, depending on the cellulose source, hydrolysis time and the enzyme loading).[16,22,27,28] The poor dispersibility of the particles restricts the characterization of the apparent particle size by dynamic light scattering and complicates statistical particle size measurements based on transmission electron microscopy (TEM) and atomic force microscopy (AFM) imaging techniques. Long cellulose fibres are clearly retained in blank reactions (Table 1 entry 4, Fig. 3e, additional images in Fig S3†). Contrastingly, cotton hydrolysed by *Tr* enzymes to the levelling off DP_n predominantly contains shorter elements, albeit poorly individualized on the TEM images (Table 1 entry 7, TEM on Fig. 3e, additional images in Fig S4†). The estimated length of the particles (150–350 nm,
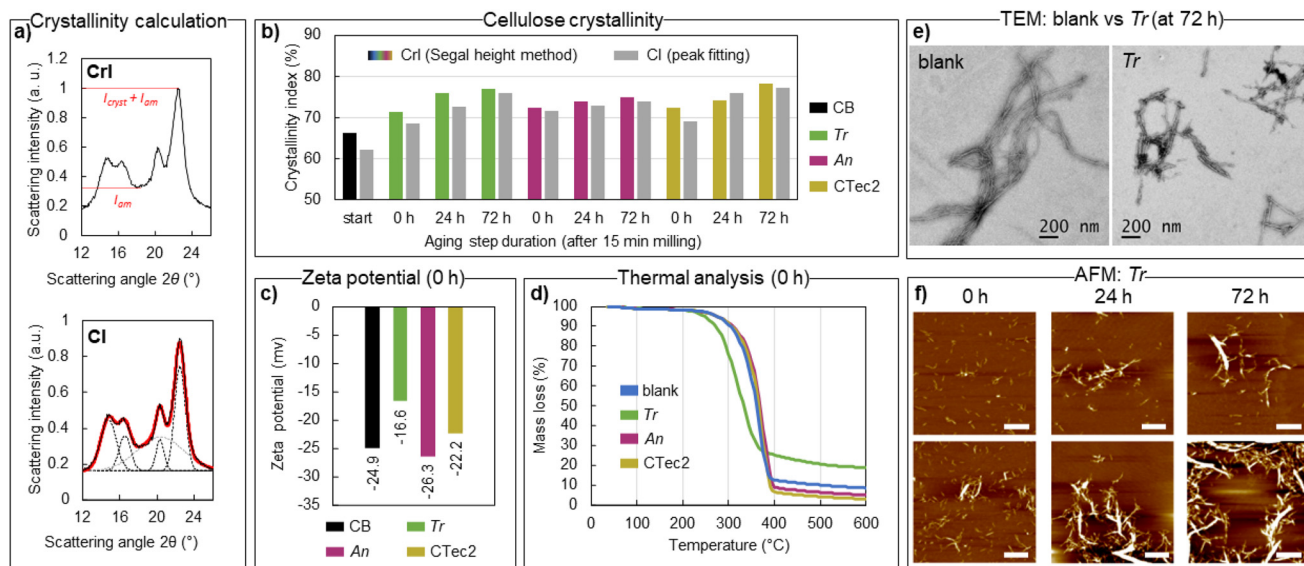
Fig. 3 Characterization of the isolated hydrolysed cellulose by X-ray diffraction (a and b), zeta potential measurements (c), thermal analysis (d), transmission electron microscopy TEM (e) and atomic force microscopy AFM (f). Panel b compiles the CrI (in colour) and CI (in grey) for the isolated hydrolysed cellulose, right after milling, and after subsequent aging for 24 or 72 h at 55 °C, by comparing *Trichoderma reesei* (*Tr*), *Aspergillus niger* (*An*) and Cellic CTec2 enzymes to the starting material (CB start), calculated as shown in panel a, based on data shown in Fig. S2.† Zeta potentials (c) and thermal analysis (d) were used to compare the isolated materials from mechanoenzymatic treatment (milled only, Table 1 entries 5, 8 and 11) with the starting material (CB) and with the blank reaction (no enzyme, Table 1 entry 2), respectively. The TEM images (e) were used to compare the cellulose isolated from a blank reaction (no enzyme) with that hydrolysed under the same reaction conditions with *Tr* cellulases (Table 1 entries 4 vs. 7). The AFM images (f) were used to compare the cellulose hydrolysed by *Tr* cellulases: right after milling (0 h) and after subsequent aging for 24 or 72 h at 55 °C. Two images of each timepoint are shown. Scale bar is 1 μm, and all images have the height scale from −10 to 10 nm.

see ESI Fig. S4†) corresponds well to that reported for CNCs obtained by sulphuric acid hydrolysis from cotton (100–300 nm).[75] Some larger fragments could be observed, which aligns with the observed increased dispersity of cellulose after hydrolysis.

The AFM images of *Tr*-hydrolyzed samples (Table 1, entries 5–7) dispersed in formic acid, one of the few solvents shown to improve the dispersion of non-charged cellulose nanocrystals,[76] reveal that individual CNCs are generated. The length distribution (150–400 nm, ESI Fig. S5†) of the particles shown in Fig. 3f (at 0 h) agrees well with the TEM data (at 72 h), showing that the nanoscale particles are present in the sample right after milling. These observations, together with bulk characterization by GPC and XRD, indicate that cellulose is transformed to nanoscale crystallites within the initial 15 minutes of milling. Limited conversion of cellulose to soluble sugars at this time point ensures that a high proportion of hydrolysed cellulose is recovered (>90%, Table 1, entries 5, 8 and 11), giving process mass intensities of 2.3 (*Tr*), 2.1 (*An*) and 2.2 (CTec2). Process mass intensity (PMI)[77] is a sustainability metric that evaluates the total input mass of materials (including reaction media) that is incorporated into the product (ESI, eqn (S3)†), with an optimal value of 1. The mechanoenzymatic approach reported herein shows a 50-fold improvement in PMI, compared to the reported in-solution enzymatic methods to produce cellulose nanomaterials (details in ESI, Table S7†), and a *ca.* 2.5-fold improvement

compared to the previously reported HefCel process.[24] However, due to the short reaction time and minimized reaction volume (0.25 h, 50 wt% solid loading), more than a 100-fold improvement in the space–time-yield (3.5–3.8 kg L⁻¹ h⁻¹) is achieved compared to the HefCel process, and more than 30 000-fold improvement over the reported in-solution methods (Table S7 and eqn (S4)†). It must be noted, however, that the reported in-solution processes often investigate the co-production of glucose and CNCs for integrated biorefineries, which maximizes the glucose production and therefore a low yield of recovered cellulose (*ca.* 10%) is reported, affecting the space–time-yield. The mechanoenzymatic approach also provides significant economic and environmental benefits compared to acid hydrolysis. The reagent cost estimate, for transforming 1 gram of starting material (cotton), comparing the mechanoenzymatic methods developed here with conventional acid hydrolysis using sulfuric,[6] hydrochloric[78–80] or phosphoric acid[81] (Table S8†), shows that the mechanoenzymatic process using *An* and CTec2 brings a 7- and 4- fold decrease in costs, respectively, compared to the cheapest sulfuric acid treatment. The process using the *Tr* enzyme matches the price of HCl hydrolysis and is only 2-fold more expensive than the sulfuric acid treatment, due to the higher enzyme loading. The phosphoric acid hydrolysis proved to have the highest reagent cost. Notably, this cost estimate does not account for the economic and environmental benefits of the mechanoenzymatic method, which arise from avoiding

equipment corrosion, avoiding the generation of corrosive wastes, avoiding hazards to personnel and avoiding the large amount of water and/or base required for the removal of the concentrated acids. The energy consumption of the used equipment (Retsch MM400 mixer mill, loaded with two 15 mL stainless steel jars) for the reaction described in Table 1, entry 5, was found to be 0.016 kW h, which is less than the energy required for 45 minutes of sulfuric acid hydrolysis[6] at 45 °C using a heating mantle with stirring (0.024 kW h). The energy consumed for hydrochloric acid[78] and phosphoric acid[81] hydrolysis carried out at 100 °C is 10–20× higher than that of the method reported herein (*ca.* 0.250 kW h and *ca.* 0.160 kW h for the 180- and 90-minute reactions, respectively). Notably, no energy is directly consumed during HCl-gas hydrolysis. For the details of the measurements of energy consumption, see ESI Table S8.†

Conclusions

We have examined the production of cellulose nanocrystals from cotton by solid-state mechanoenzymatic approaches using three commercially available cellulase systems from *Trichoderma reesei*, *Aspergillus niger* and a Cellic CTec2 cellulase blend. All applied cellulase systems lead to a rapid drop in the degree of polymerization near the levelling-off degree of polymerization of cotton and to a sharp increase in the crystallinity of cellulose, during a short 15 minutes mechanoenzymatic reaction. This indicates that the bulk material is quickly transformed to cellulose nanomaterials, at a space–time-yield of 3.5–3.8 kg L^{-1}. Subsequent aging of the solid reaction mixture at 55 °C did not further decrease the DP_n, but resulted in higher material losses due to the increased production of glucose. *An* cellulases appear particularly suitable for this process, leading to a low DP_n at a significantly lower enzyme loading (0.085 wt%) compared to *Tr* and CTec2 cellulases (1.56 wt% and 0.3 wt%, respectively). Utilizing renewable catalysts (enzymes) and avoiding much of the waste and energy lost in heating dilute aqueous solutions, the mechanoenzymatic method for producing cellulose nanomaterials is highly efficient (PMI 2.1–2.3) and offers notable economic and environmental benefits.

Experimental

The following is a concise overview of the materials and methods used. Full experimental details are included in the ESI file.†

Materials

Cotton was purchased as non-sterile raw cotton balls (CB) along with Whatman type 1 filter paper (FP). Both materials were milled to powders using a Thomas Scientific Wiley Mini Mill 475-A equipped with a 30-mesh screen and thereafter used in reactions without further purification. The cellulases from *Trichoderma reesei*, *Aspergillus niger* and the CTec2® blend were purchased from Sigma-Aldrich and had a comparable activity of 1–2 U mg^{-1} based on the producer's specifications and in the hydrolysis assay of microcrystalline cellulose (Sigma Aldrich, average 51 μm particles). The enzymes were stored at 4 °C. Buffers were prepared using Milli-Q water with a conductivity of 1.8 μS cm^{-1} at 25 °C, and included 0.02 wt% of sodium azide as a bacteriostatic preservative.

Methods

In a typical reaction, pre-milled cotton powder (400 mg) was weighed into a 15 mL stainless steel jar with a 4 g stainless steel ball, to which the commercial enzyme preparation (either 20 mg of *Trichoderma reesei*, 20 mg of *Aspergillus niger* or 20 mg (17.4 μL) of the CTec2® blend and buffer (420 μL)) was added, bringing the total liquid-to-solid ratio to 1.0 μL mg^{-1}, corresponding to a solid loading of 50% w/w. The milling jars were then closed and set to mill at 25 Hz for 15 minutes. The resulting uniform solids were aliquoted into 1.5 mL Eppendorf tubes affording analysis samples for glucose assays (20–30 mg) and for recovered cellulose isolation (200 mg) at different time points: immediately after milling, after subsequent aging for 24 h at 55 °C, and after subsequent aging for 72 h at 55 °C. The commercial Glucose (HK) Assay Reagent (purchased from Sigma Aldrich) was used to quantify glucose in the reaction mixtures. An aliquot of 200–250 mg of the reaction mixture (solid content: 48–50%) was taken at the end of the reaction, suspended in 1 wt% washing buffer (50 mM citrate buffer, adjusted with NaOH to pH 10) and incubated for 1 h with gentle magnetic stirring at 100 rpm to remove the enzyme. Thereafter, the solids were collected by vacuum filtration and washed on a 0.22 μm polypropylene or nylon membrane, once with the washing buffer and three times with Milli-Q water. The solids were collected from the membrane by rinsing with Milli-Q water into a Falcon tube and freeze dried. Some loss of solids could not be avoided upon flushing of the membrane, which is reflected in the recovery% of cellulose. The weight of the dry solids was recorded, from which the recovery% was calculated as follows:

$$\text{Recovery\%} = \frac{m(\text{dry solids, mg})}{m(\text{aliquot, mg}) \times 0.48} \times 100\%$$

Specific reaction conditions, together with the hydrolysis yields, are compiled in Table S1.† 50 ± 5 mg of the washed and freeze-dried recovered cellulose samples were prepared for GPC analysis by the water–acetone–*N*,*N*-dimethylacetamide (DMAc) solvent exchange procedure, followed by dissolution in 90 g L^{-1} LiCl/DMAc, analysis at 1 mg mL^{-1} against Pullulan standards on a Dionex UltiMate 3000 HPLC system, and elution with 9 g^{-1} LiCl/DMAc at a flow rate of 0.75 mL min^{-1}. About 15–20 mg of the dry recovered cellulose samples was used for collecting wide-angle X-ray scattering (WAXS) data using a Xeuss 3.0 C scattering device (Xenocs, France). Crystallinity changes were estimated based on CrI, calculated according to the empirical Segal peak height method,[70] and CI was calculated based on peak fitting. Atomic Force Microscopy

(AFM) images were recorded on a Bruker MultiMode8 instrument, from samples dispersed at 1 wt% in formic acid and spin-coated on UV-cleaned silicon wafers. Formic acid adsorbs onto the surfaces of the CNCs and disrupts the hydrogen bonds between aggregated particles, which enables the dispersion of non-charged CNCs.[76] A small amount of formate ester moieties may also be formed on the surface of CNCs,[76] which may also facilitate the dispersion in formic acid. Zeta potentials were measured on the Malvern Zetasizer, and thermal analysis was carried out with the Netzsch STA 449 F3 Jupiter system. Transmission electron microscopy imaging was performed on an FEI Tecnai 12 microscope at an acceleration voltage of 120 kV. A Thermo Scientific Flash Smart CHNS elemental analyzer was used to qualitatively confirm the presence of protein impurities in washed and freeze-dried recovered cellulose samples. Changes in the surface charge of recovered cellulose were probed by zeta potential measurements using a Malvern Zetasizer Nano ZS90. Further details are provided in the ESI.†

Author contributions

The authors have contributed to the following tasks: S.K.: conceptualization, investigation (data acquisition and analysis), writing the original draft and funding acquisition; I.S.-H. investigation (thermal analysis data acquisition and analysis); M.K. and E.K.: investigation (data analysis), supervision, and writing (review and editing).

Data availability

The data supporting this article have been included as part of the ESI.† The ESI† file compiles detailed information on the materials, methods, and equipment used. It also contains the description of the equations used for calculations (eqn (S1)–(S4)), ESI Fig. (S1–S3) and Tables (S1–S6)† referenced in the manuscript.

Conflicts of interest

There are no conflicts to declare.

References

1 D. Klemm, E. D. Cranston, D. Fischer, M. Gama, S. A. Kedzior, D. Kralisch, F. Kramer, T. Kondo, T. Lindström, S. Nietzsche, K. Petzold-Welcke and F. Rauchfuß, *Mater. Today*, 2018, **21**, 720–748.

2 J. A. Shatkin, T. H. Wegne, E. M. T. Bilek and J. Cowie, *Tappi J.*, 2014, **13**, 9–16.

3 F. A. G. S. Silva, F. Dourado, M. Gama and F. Poças, *Nanomaterials*, 2020, **10**, 2041.

4 S. S. Ahankari, A. R. Subhedar, S. S. Bhadauria and A. Dufresne, *Carbohydr. Polym.*, 2021, **255**, 117479.

5 O. Nechyporchuk, M. N. Belgacem and J. Bras, *Ind. Crops Prod.*, 2016, **93**, 2–25.

6 M. S. Reid, M. Villalobos and E. D. Cranston, *Langmuir*, 2017, **33**, 1583–1598.

7 G. Delepierre, O. M. Vanderfleet, E. Niinivaara, B. Zakani and E. D. Cranston, *Langmuir*, 2021, **37**, 8393–8409.

8 M. Jonoobi, R. Oladi, Y. Davoudpour, K. Oksman, A. Dufresne, Y. Hamzeh and R. Davoodi, *Cellulose*, 2015, **22**, 935–969.

9 O. M. Vanderfleet and E. D. Cranston, *Nat. Rev. Mater.*, 2021, **6**, 124–144.

10 P. Squinca, S. Bilatto, A. C. Badino and C. S. Farinas, *ACS Sustainable Chem. Eng.*, 2020, **8**, 2277–2286.

11 P. Squinca, S. Bilatto, A. C. Badino and C. S. Farinas, *Carbohydr. Polym. Technol. Appl.*, 2022, **3**, 100212.

12 C. R. Bauli, D. B. Rocha, S. A. de Oliveira and D. S. Rosa, *J. Cleaner Prod.*, 2019, **211**, 408–416.

13 R. S. S. Teixeira, A. S. A. Da Silva, J. H. Jang, H. W. Kim, K. Ishikawa, T. Endo, S. H. Lee and E. P. S. Bon, *Carbohydr. Polym.*, 2015, **128**, 75–81.

14 C. R. Bauli, D. B. Rocha and D. D. S. Rosa, *SN Appl. Sci.*, 2019, **1**, 774.

15 P. B. Filson, B. E. Dawson-Andoh and D. Schwegler-Berry, *Green Chem.*, 2009, **11**, 1808.

16 J. De Aguiar, T. J. Bondancia, P. I. C. Claro, L. H. C. Mattoso, C. S. Farinas and J. M. Marconcini, *ACS Sustainable Chem. Eng.*, 2020, **8**, 2287–2299.

17 S. R. Anderson, D. Esposito, W. Gillette, J. Y. Zhu, U. Baxa and S. E. McNeil, *Tappi J.*, 2014, **13**, 35–42.

18 G. A. Siqueira, I. K. R. Dias and V. Arantes, *Int. J. Biol. Macromol.*, 2019, **133**, 1249–1259.

19 A. A. Domingues, F. V. Pereira, M. R. Sierakowski, O. J. Rojas and D. F. S. Petri, *Cellulose*, 2016, **23**, 2421–2437.

20 J. M. Yarbrough, R. Zhang, A. Mittal, T. Vander Wall, Y. J. Bomble, S. R. Decker, M. E. Himmel and P. N. Ciesielski, *ACS Nano*, 2017, **11**, 3101–3109.

21 P. Satyamurthy, P. Jain, R. H. Balasubramanya and N. Vigneshwaran, *Carbohydr. Polym.*, 2011, **83**, 122–129.

22 X. Tong, W. Shen, X. Chen, M. Jia and J. Roux, *J. Appl. Polym. Sci.*, 2020, **137**, 48407.

23 X. Q. Chen, G. X. Pang, W. H. Shen, X. Tong and M. Y. Jia, *Carbohydr. Polym.*, 2019, **207**, 713–719.

24 J. Pere, T. Tammelin, P. Niemi, M. Lille, T. Virtanen, P. A. Penttilä, P. Ahvenainen and S. Grönqvist, *ACS Sustainable Chem. Eng.*, 2020, **8**, 18853–18863.

25 J. T. Xu, X. Q. Chen, W. H. Shen and Z. Li, *Carbohydr. Polym.*, 2021, **256**, 117493.

26 R. S. A. Ribeiro, N. Bojorge and N. Pereira, *Biotechnol. Appl. Biochem.*, 2020, **67**, 366–374.

27 B. Alonso-Lerma, L. Barandiaran, L. Ugarte, I. Larraza, A. Reifs, R. Olmos-Juste, N. Barruetabeña, I. Amenabar, R. Hillenbrand, A. Eceiza and R. Perez-Jimenez, *Commun. Mater.*, 2020, **1**, 57.

28 B. Alonso-Lerma, I. Larraza, L. Barandiaran, L. Ugarte, A. Saralegi, M. A. Corcuera, R. Perez-Jimenez and A. Eceiza, *Carbohydr. Polym.*, 2021, **254**, 117478.

29 F. Hammerer, L. Loots, J. Do, J. P. D. Therien, C. W. Nickels, T. Friščić and K. Auclair, *Angew. Chem., Int. Ed.*, 2018, **57**, 2621–2624.

30 F. Hammerer, S. Ostadjoo, K. Dietrich, M.-J. J. Dumont, L. F. Del Rio, T. Friščić and K. Auclair, *Green Chem.*, 2020, **22**, 3877–3884.

31 S. Ostadjoo, F. Hammerer, K. Dietrich, M.-J. Dumont, T. Friščić and K. Auclair, *Molecules*, 2019, **24**, 4206.

32 F. Hammerer, S. Ostadjoo, T. Friščić and K. Auclair, *ChemSusChem*, 2020, **13**, 106–110.

33 M. Käldström, N. Meine, C. Farès, R. Rinaldi and F. Schüth, *Green Chem.*, 2014, **16**, 2454–2462.

34 J. Hilgert, N. Meine, R. Rinaldi and F. Schüth, *Energy Environ. Sci.*, 2013, **6**, 92–96.

35 A. Shrotri, L. K. Lambert, A. Tanksale and J. Beltramini, *Green Chem.*, 2013, **15**, 2761–2768.

36 M. Kessler and R. Rinaldi, *Front. Chem.*, 2022, **9**, 816553.

37 Y. Dong, L. Schneider, T. Hu, M. Jaakkola, J. Holm, J. M. Leveque and U. Lassi, *Biomass Bioenergy*, 2016, **86**, 36–42.

38 Y. Yu, Y. Long and H. Wu, *Energy Fuels*, 2016, **30**, 1571–1578.

39 L. Schneider, J. Haverinen, M. Jaakkola and U. Lassi, *Bioresour. Technol.*, 2017, **234**, 1–7.

40 P. Dornath, H. J. Cho, A. Paulsen, P. Dauenhauer and W. Fan, *Green Chem.*, 2015, **17**, 769–775.

41 Q. Zhang and F. Jérôme, *ChemSusChem*, 2013, **6**, 2042–2044.

42 S. M. Hick, C. Griebel, D. T. Restrepo, J. H. Truitt, E. J. Buker, C. Bylda and R. G. Blair, *Green Chem.*, 2010, **12**, 468–447.

43 T. Friščić, C. Mottillo and H. M. Titi, *Angew. Chem., Int. Ed.*, 2020, **59**, 1018–1029.

44 S. Kaabel, T. Friščić and K. Auclair, *ChemBioChem*, 2020, **21**, 742–758.

45 C. C. Piras, S. Fernández-Prieto and W. M. De Borggraeve, *Nanoscale Adv.*, 2019, **1**, 937–947.

46 J. Gröndahl, K. Karisalmi and J. Vapaavuori, *Soft Matter*, 2021, **17**, 9842–9858.

47 T. Yang, X. Li, Y. Guo, S. Peng, G. Liu and J. Zhao, *Ind. Crops Prod.*, 2020, **155**, 112755.

48 S. Cui, S. Zhang, S. Ge, L. Xiong and Q. Sun, *Ind. Crops Prod.*, 2016, **83**, 346–352.

49 M. Qian, H. Lei, E. Villota, Y. Zhao, C. Wang, E. Huo, Q. Zhang, W. Mateo and X. Lin, *Chem. Eng. Process.*, 2021, **160**, 108292.

50 Q. Zhang, Z. Lu, C. Su, Z. Feng, H. Wang, J. Yu and W. Su, *Bioresour. Technol.*, 2021, **331**, 125015.

51 M. S. Reid, M. Villalobos and E. D. Cranston, *Langmuir*, 2017, **33**, 1583–1598.

52 O. M. Vanderfleet and E. D. Cranston, *Nat. Rev. Mater.*, 2021, **6**, 124–144.

53 M. Pérez-Venegas and E. Juaristi, *ChemSusChem*, 2021, **14**, 2682–2688.

54 J. Arciszewski and K. Auclair, *ChemSusChem*, 2022, **15**, e202102084.

55 T. Friščić, D. G. Reid, I. Halasz, R. S. Stein, R. E. Dinnebier and M. J. Duer, *Angew. Chem., Int. Ed.*, 2010, **49**, 712–715.

56 L. Chen, M. Regan and J. Mack, *ACS Catal.*, 2016, **6**, 868–872.

57 J. Andersen and J. Mack, *Green Chem.*, 2018, **20**, 1435–1443.

58 S. K. Brady, S. Sreelatha, Y. Feng, S. P. S. Chundawat and M. J. Lang, *Nat. Commun.*, 2015, **6**, 10149.

59 Y. Shang, R. Su, R. Huang, Y. Yang, W. Qi, Q. Li and Z. He, *Appl. Microbiol. Biotechnol.*, 2014, **98**, 5765–5774.

60 B. Henrissat, *Cellulose*, 1994, **1**, 169–196.

61 J. Pere, M. Siika-aho, J. Buchert and L. Viikari, *Tappi J.*, 1995, **78**, 71–78.

62 J. Rahikainen, O. Mattila, T. Maloney, V. Lovikka, K. Kruus, A. Suurnäkki and S. Grönqvist, *Cellulose*, 2020, **27**, 5311–5322.

63 S. Grönqvist, T. Kamppuri, T. Maloney, M. Vehviläinen, T. Liitiä and A. Suurnäkki, *Cellulose*, 2015, **22**, 3981–3990.

64 P. Spiliopoulos, S. Spirk, T. Ppaakkonen, M. Viljanen, K. Svedstrom, L. Pitkanen, M. Awais and E. Kontturi, *Biomacromolecules*, 2021, **22**, 1399–1405.

65 K. Igarashi, M. Wada, R. Hori and M. Samejima, *FEBS J.*, 2006, **273**, 2869–2878.

66 P. Väljamäe, V. Sild, G. Pettersson and G. Johansson, *Eur. J. Biochem.*, 1998, **253**, 469–475.

67 J. P. D. Therien, F. Hammerer, T. Friščić and K. Auclair, *ChemSusChem*, 2019, **12**, 3481–3490.

68 S. Kaabel, J. P. D. Therien, C. E. Deschênes, D. Duncan, T. Friščić and K. Auclair, *Proc. Natl. Acad. Sci. U. S. A.*, 2021, **118**, e2026452118.

69 S. Kaabel, J. Arciszewski, T. H. Borchers, J. P. D. Therien, T. Friščić and K. Auclair, *ChemSusChem*, 2023, **16**, e202201613.

70 L. Segal, J. J. Creely, A. E. Martin and C. M. Conrad, *Text. Res. J.*, 1959, **29**, 786–794.

71 K. S. Salem, N. K. Kasera, M. A. Rahman, H. Jameel, Y. Habibi, S. J. Eichhorn, A. D. French, L. Pal and L. A. Lucia, *Chem. Soc. Rev.*, 2023, **52**, 6417–6446.

72 P. Ahvenainen, I. Kontro and K. Svedström, *Cellulose*, 2016, **23**, 1073–1086.

73 M. Kröger, O. Badara, T. Pääkkönen, I. Schlapp-Hackl, S. Hietala and E. Kontturi, *Biomacromolecules*, 2023, **24**, 1318–1328.

74 T. J. Bondancia, C. Florencio, G. S. Baccarin and C. S. Farinas, *Int. J. Biol. Macromol.*, 2022, **207**, 299–307.

75 S. Elazzouzi-Hafraoui, Y. Nishiyama, J.-L. Putaux, L. Heux, F. Dubreuil and C. Rochas, *Biomacromolecules*, 2008, **9**, 57–65.

76 O. van der Berg, J. R. Capadona and C. Weder, *Biomacromolecules*, 2007, **8**, 1353–1357.

77 C. Jimenez-Gonzalez, C. S. Ponder, Q. B. Broxterman and J. B. Manley, *Org. Process Res. Dev.*, 2011, **15**, 912–917.

78 H. Yu, Z. Qin, B. Liang, N. Liu, Z. Zhou and L. Chen, *J. Mater. Chem. A*, 2013, **1**, 3938–3944.

79 E. Kontturi, A. Meriluoto, P. A. Penttilä, N. Baccile, J. Malho, A. Potthast, T. Rosenau, J. Ruokolainen, R. Serimaa, J. Laine and H. Sixta, *Angew. Chem., Int. Ed.*, 2016, **55**, 14455–14458.

80 T. Pääkkönen, P. Spiliopoulos, A. Knuts, K. Nieminen, L.-S. Johansson, E. Enqvist and E. Kontturi, *React. Chem. Eng.*, 2018, **3**, 312–318.

81 S. Camarero Espinosa, T. Kuhnt, E. J. Foster and C. Weder, *Biomacromolecules*, 2013, **14**, 1223–1230.